RAP80 and BRCA1 PARsylation protect chromosome integrity by preventing retention of BRCA1-B/C complexes in DNA repair foci

Jekaterina Vohhodina[a,b], Kimberly J. Toomire[a,b,1], Sarah A. Petit[a,b,2], Goran Micevic[c], Geeta Kumari[a,b], Vladimir V. Botchkarev Jr[a,b], Zhe Li[b,d], David M. Livingston[a,b,e,3], and Yiduo Hu[f,3]

[a]Department of Cancer Biology, Dana-Farber Cancer Institute, Boston, MA 02215; [b]Division of Genetics, Brigham and Women's Hospital, Harvard Medical School, Boston, MA 02115; [c]Department of Dermatology, Yale School of Medicine, Yale University, New Haven, CT 06510; [d]Department of Medicine, Harvard Medical School, Boston, MA 02115; [e]Department of Genetics, Harvard Medical School, Boston, MA 02115; and [f]Department of Medicine, Yale School of Medicine, Yale University, New Haven, CT 06510

BRCA1 promotes error-free, homologous recombination-mediated repair (HRR) of DNA double-stranded breaks (DSBs). When excessive and uncontrolled, BRCA1 HRR activity promotes illegitimate recombination and genome disorder. We and others have observed that the BRCA1-associated protein RAP80 recruits BRCA1 to postdamage nuclear foci, and these chromatin structures then restrict the amplitude of BRCA1-driven HRR. What remains unclear is how this process is regulated. Here we report that both BRCA1 poly-ADP ribosylation (PARsylation) and the presence of BRCA1-bound RAP80 are critical for the normal interaction of BRCA1 with some of its partners (e.g., CtIP and BACH1) that are also known components of the aforementioned focal structures. Surprisingly, the simultaneous loss of RAP80 and failure therein of BRCA1 PARsylation results in the dysregulated accumulation in these foci of BRCA1 complexes. This in turn is associated with the intracellular development of a state of hyper-recombination and gross chromosomal disorder. Thus, physiological RAP80-BRCA1 complex formation and BRCA1 PARsylation contribute to the kinetics by which BRCA1 HRR-sustaining complexes normally concentrate in nuclear foci. These events likely contribute to aneuploidy suppression.

BRCA1 | PARsylation | RAP80 | HRR | IRIF

Homologous recombination-mediated repair (HRR) is a major DNA repair process that is required for cell survival and the suppression of genomic instability after DNA damage. Normally, HRR is an error-free process in which faithful recombination occurs between sister chromatids (1, 2). In contrast, illegitimate recombination between nonallelic sequences can result in deleterious genome rearrangements in both germ line and somatic cell DNA (3). A number of proteins function during the HRR process or at the interface between HRR and other DNA repair processes to suppress illegitimate recombination. A number of them, including BLM (4), FANCM/MPH1 (5), FBH1 (6), PARI (7), RECQL5 (8), and RTEL (9), suppress HRR-induced chromosome instability, genome rearrangement, and, in some cases, cancer development.

BRCA1 is a major HRR support protein (10, 11). Working together with certain partner proteins, including RAD51, CtIP, and BACH1 (also known as FANCJ/BRIP1), it promotes double-strand break (DSB) end resection, proper HRR progression, and recombinational fidelity (12–14). However, BRCA1 HRR function must be tightly controlled to prevent illegitimate recombination and genomic instability (15–18). In this regard, RAP80, a major BRCA1 partner, functions to maintain normal concentrations of BRCA1 in ionizing radiation (IR)-induced foci (IRIF). This process leads to suppression of excessive DNA end resection, which can result in a hyper-HRR phenotype (15, 16, 19, 20).

We have also found that PARP1 promotes PARsylation of the BRCA1 DNA-binding domain and physiologically down-modulates BRCA1's DNA binding and HRR activity. This process is important for chromosome integrity maintenance after cells incur IR-induced DNA damage (21).

In light of these findings, we asked how these two HRR regulatory mechanisms—PARP1-driven BRCA1 PARsylation and RAP80 complex-mediated suppression of end resection—are operationally related to one another. Our results show that, unexpectedly, after a combination of BRCA1 PARsylation failure and RAP80 depletion, BRCA1 persists in IRIF together with its pro-HRR partners, CtIP and BACH1. This combinatorial effect was associated with an even greater amplitude of HRR than arose after either perturbation, alone, as well as the development of overt chromosomal instability. Thus, BRCA1 PARsylation and normal operation of the RAP80 complex together ensure that BRCA1 HRR operates at physiological amplitude and thereby contributes to the maintenance of genome integrity.

Significance

Normally, BRCA1 promotes physiological, error-free homologous recombination repair (HRR) of damaged DNA and genome stability. In contrast, excessive, deregulated HRR can lead to genome instability. The BRCA1-binding protein RAP80 restricts HRR amplitude and genome instability, at least in part by manifesting polyubiquitin and poly-ADP-ribose binding activities in postdamage nuclear foci. Although how these processes operate in detail remains unknown, we find that simultaneous defects in RAP80/BRCA1 complex formation and in BRCA1 poly-ADP-ribosylation result in the persistent accumulation of BRCA1-containing complexes in nuclear foci that also contain CtIP and BACH1. These effects lead to excessive HRR, chromosomal hyper-recombination, and gross chromosomal abnormalities.

Results and Discussion

BRCA1 PARsylation and RAP80 Each Support Optimal HRR Regulation through Nonredundant Mechanisms.

Using the I-SceI HRR reporter system in U2OS cells (22), we and others have shown that depletion of RAP80 or certain RAP80 partner proteins (ABRAXAS [also known as ABRA1] and BRCC36) results in an elevated HRR amplitude and gross chromosomal instability (15, 16, 23, 24). Given that BRCA1 PARsylation is required for maintaining the normal integrity of RAP80-BRCA1 complexes, normal HRR amplitude, and chromosome stability (21), we analyzed the effects of RAP80 depletion on HRR in cells expressing either BRCA1-WT or BRCA1-D5 (a stable, full-length BRCA1 mutant except for deletion of an 8-residue sequence that is required for BRCA1 PARsylation) (21). Consistent with our previous observations, cells expressing BRCA1-D5 but not the WT protein exhibited significantly higher HRR amplitude compared with BRCA1-WT–expressing cells. The level was comparable to that detected in RAP80-depleted cells (Fig. 1 A and B). In addition, depletion of RAP80 in BRCA1-D5–expressing cells resulted in even greater HRR activity than was detected following either perturbation alone (Fig. 1A).

Similar HRR effects were also observed when RAP80 was codepleted in PARP1-depleted cells or in cells exposed to olaparib, a PARP1/2 inhibitor (25) that has been approved for treating BRCA1 or BRCA2 mutated breast, ovarian, and pancreatic cancers. It was given at a concentration (30 nM) sufficient to disrupt both BRCA1 PARsylation and HRR regulation without eliciting significant cytotoxicity or affecting cell cycling (*SI Appendix*, Fig. S1 A–C) (21). These results and the aforementioned findings imply that BRCA1 PARsylation and RAP80 together regulate HRR function through nonredundant mechanisms, at least when HRR at a single I-SceI–induced DSB was assessed.

We also measured HRR activity in BRCA1-WT– and BRCA1-D5–expressing cells that were codepleted of 53BP1, an important mediator of nonhomologous end-joining capable of interfering with BRCA1 HRR activity. Inactivation of 53BP1 leads to increased HRR in part through the activation of CtIP and thereby of DSB end resection. Moreover, 53BP1 nullizygosity rescues embryonic lethality in BRCA1-null mice, thus highlighting the interplay between 53BP1 and BRCA1 in the control of DSB repair (26, 27). Similar to RAP80 depletion combined with BRCA1-D5 substitution for BRCA1-WT expression, 53BP1 depletion in cells expressing BRCA1-D5 resulted in elevated HRR activity above that arising from either single perturbation, thereby emphasizing the importance of both BRCA1 PARsylation and 53BP1 function in the maintenance of physiological BRCA1-driven HRR (*SI Appendix*, Fig. S2 A and B). Interestingly, RAP80 depletion did not lead to a further increase of HRR in 53BP1-depleted cells, suggesting that RAP80 works downstream of 53BP1, as expected given that 53BP1 prevents the resection of DSBs. However, expression of BRCA1-D5 did lead to a further increase of HRR in 53BP1-depleted cells, which further implies that BRCA1 PARsylation and RAP80 work nonredundantly to suppress HRR.

We next examined the impact of RAP80 depletion on radiation-induced chromosome instability in cells expressing BRCA1-WT and in other cells expressing non-PARsylatable BRCA1-D5 in place of the WT protein. We found that cells expressing BRCA1-D5 instead of WT accumulated significant numbers of radial structures and complex chromosome rearrangements (i.e., rearrangements involving three or more chromosomes) shortly after DNA damage. These rearranged chromosomes are largely products of excessive, unregulated HRR activity in these cells (21). Since RAP80 depletion in BRCA1-D5–expressing cells resulted in a further increase in HRR activity (Fig. 1A), we expected to observe a corresponding increase in chromosome instability in
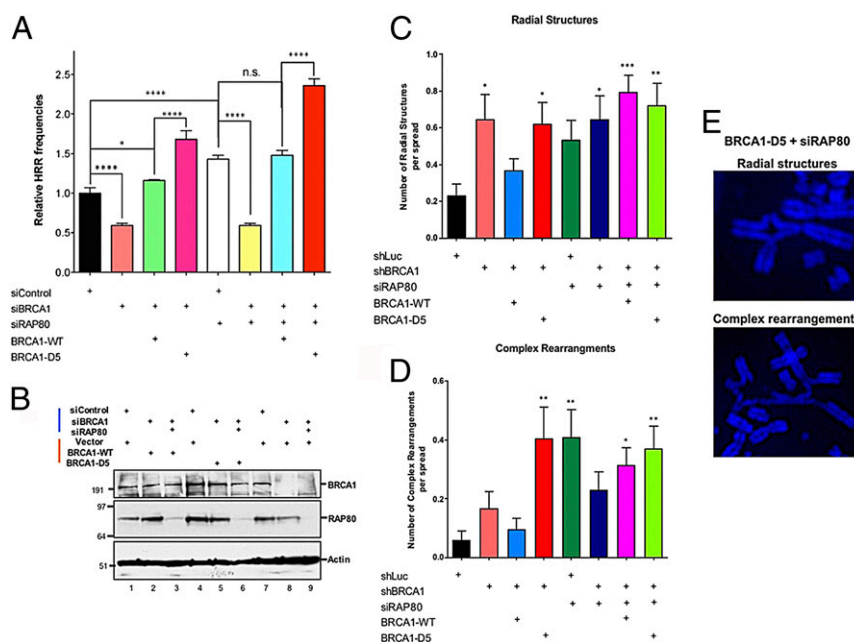
Fig. 1. BRCA1 PARsylation and RAP80 are required for normal HRR tuning and chromosome integrity control. (A) Results of HRR assays of U2OS cells expressing siRNA-resistant HA-BRCA1-WT or HA-BRCA1-D5 and transfected with control siRNA or siRNA targeting endogenous BRCA1 or RAP80. The HRR frequencies of control samples were normalized to 1. Experiments were performed in triplicate, and error bars indicate SD. *P < 0.05; **P < 0.01; ***P < 0.001; ****P < 0.0001; n.s., not statistically significant. (B) Western blots in cells described in A showing detection of both endogenous and HA-tagged BRCA1, RAP80, and actin. (C and D) Effects of RAP80 depletion on chromosome stability in cells cotransduced with shLuc, shBRCA1, or shBRCA1 and shRNA-resistant BRCA1-WT or BRCA1-D5. (C) Graph showing the frequencies of radial structures. (D) A graph showing the frequencies of complex rearrangements. Between 40 and 70 spreads were counted in each category of cells, and error bars indicate the SEM. *P < 0.05; **P < 0.01; ***P < 0.001. (E) Representative images (60× magnification) of chromosome aberrations (radial structures and complex rearrangements) in cells expressing siRNA-resistant HA-BRCA1-D5 and transfected with siRNA targeting endogenous BRCA1 and RAP80.

these cells; however, this was not the case. RAP80 depletion, alone or combined with BRCA1-D5 expression, led to comparable levels of radial and complex rearrangements. Moreover, these levels were comparable to those observed after BRCA1-D5 expression alone, although they were also significantly higher than those in control cells (Fig. 1 *C–E*).

A combination of RAP80 depletion and BRCA1-D5 substitution for endogenous BRCA1-WT conceivably has the potential to engender additional chromosome instability in at least some targeted cells while at the same time blocking their cell cycle progression. This could result in a failure to detect a more extreme chromosomal phenotype when the two perturbations coexist. Alternatively, there may be a limit to the amount of chromosomal instability that can be tolerated by elevating HRR activity, which might lead to cell death if sufficiently elevated. These considerations notwithstanding, the aforementioned results indicate that both RAP80 and normal BRCA1 PARsylation are required for optimal HRR control, possibly operating by different mechanisms given their different innate biochemical functions.

Dynamics of BRCA1 PARsylation in Response to DNA Damage and RAP80 Function. To further delineate the tempo of BRCA1 PARsylation, we also examined the dynamics of this modification over time following the introduction of DNA damage via IR. More specifically, this was accomplished in cells incubated in the absence versus the presence of the PARP inhibitor olaparib and with or without RAP80 depletion (*SI Appendix*, Fig. S3 *A* and *B*). The data revealed the existence of two periods of significant BRCA1 PARsylating activity: an earlier period that peaked between 15 and 30 min post-IR and a later one that peaked at ~2 h post-IR and persisted for up to 8 h. Both were suppressed by olaparib (*SI Appendix*, Fig. S3 *A* and *B*).

Interestingly, RAP80 depletion led to a diminution of the earlier period of BRCA1 PARsylating activity but not of the later period, suggesting that different BRCA1 PARsylation-regulating mechanisms operate during these different postdamage intervals (*SI Appendix*, Fig. S3 *A* and *B*). The later RAP80- independent BRCA1 PARsylation interval is particularly interesting, since the majority of DNA damage-associated poly-ADP-ribosylation is known to occur within seconds to minutes after DNA damage and to be short-lived due to rapid de-PARsylation (28). Thus, in one model these results are consistent with the possibility that BRCA1 PARsylation and de-PARsylation contribute to the respective assembly and dissociation of BRCA1-containing complexes in IRIF in a finely organized temporal order following the onset of DNA damage (see the model in Fig. 5).

Inhibition of BRCA1 PARsylation "Reverses" the Loss of BRCA1 from IRIF in the Absence of RAP80. An earlier model depicted RAP80 complexes recruiting BRCA1 to focal sites of DNA damage (i.e., IRIF) (11, 29–31). However, we and others were unable to show that RAP80 recruits a majority of the ambient BRCA1 to IRIF per se (15, 16, 21, 32). Furthermore, RAP80 loss resulted in only a gradual diminution of BRCA1 from IRIF rather than its acute and complete loss, and this loss occurred primarily at late time points (i.e., hours) after the onset of DNA damage (15, 23, 32).

There were fewer BRCA1-immunostained IRIF in these RAP80-depleted cells compared with control cells (15). However, a majority of these IRIF contained BRCA1-bound CtIP or BACH1, despite being RAP80-free. This observation implies that ongoing HRR activity, perhaps even excessive HRR activity, such as might occur following inappropriate end resection, is afoot in these structures (15).

Since BRCA1 PARsylation is required to maintain the stability of BRCA1-RAP80 complexes (21), we asked whether inhibiting this modification perturbs the formation and/or retention of BRCA1-containing complexes in IRIF. Specifically, we incubated

cells in medium containing olaparib vs. drug-free medium. Olaparib failed to alter the kinetics of BRCA1-containing IRIF formation or the colocalization in these structures of BRCA1 and RAP80 (Fig. 2 *A* and *B*, compare black and blue lines). Thus, inhibiting PARsylation with olaparib alone did not alter the recruitment and maintenance of BRCA1 in IRIF.

Also consistent with previous findings (15), RAP80 depletion led to a significant loss of BRCA1 IRIF, but mostly at late time points after IR (Fig. 2*B*, 6 to 16 h, green line). In contrast, when RAP80-depleted cells were simultaneously exposed to olaparib, distinct intensely staining BRCA1 IRIF were unexpectedly detected in the majority of cells, and the percentage of these BRCA1 IRIF-positive cells reached a level comparable to that of unperturbed control cells (Fig. 2 *A* and *B*). Therefore, the loss of BRCA1 from IRIF in the absence of RAP80 was reversed by inhibiting PARsylation. These "restored" BRCA1 foci persisted for up to 16 h post-IR, comparable to the kinetics of IRIF detected in untreated cells (Fig. 2*B*).

Given these findings, one might speculate that olaparib-induced trapping of PARP1 on DNA (33, 34) results in DNA damage that leads to BRCA1 chromatin recruitment independent of RAP80. Therefore, we compared the functionality of BRCA1-WT and the non-PARsylatable mutant, BRCA1-D5 (21), in IRIF. At 8 h after IR treatment of otherwise unperturbed cells, both proteins (BRCA1-WT and BRCA1-D5) had concentrated in distinct foci that also contained RAP80 (*SI Appendix*, Fig. S4*A*). In contrast, at the same time point in RAP80-depleted cells, BRCA1-WT had already largely dispersed from IRIF, while BRCA1-D5 was still concentrated in these foci in most of the cells (*SI Appendix*, Fig. S4 *A* and *B*). Again, BRCA1-containing foci were seemingly "restored" in the BRCA1-D5 mutant cells by these combined perturbations.

These findings imply that BRCA1 PARsylation is required for the exit of BRCA1 from the majority of IRIF in the absence of RAP80 at late time points after DNA damage. However, if RAP80 were depleted from cells and the BRCA1 PARsylation process were defective, BRCA1 could persist abnormally in IRIF in a setting conducive to the induction of genome instability. These results reinforce the view that RAP80 is required to support the physiological maintenance over time of BRCA1 in
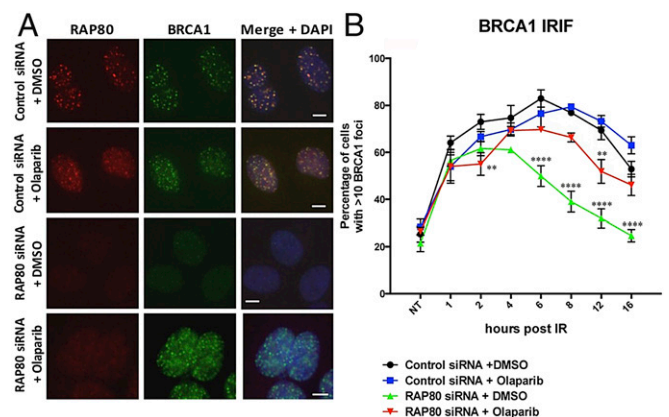
Fig. 2. PARsylation inhibition restores BRCA1 to RAP80-free IRIF. (*A*) Representative images showing RAP80 and BRCA1 focus (i.e., IRIF) formation. U2OS cells were transfected with control siRNA + DMSO, control siRNA + 30 nM olaparib, *RAP80* siRNA + DMSO, or *RAP80* siRNA + 30 nM olaparib for 48 h, then irradiated and allowed to recover for 8 h before being processed for RAP80 or BRCA1 immunostaining. (Scale bars, 10 μm.) (*B*) Effects of PARP1 inhibition and RAP80 depletion on the kinetics of BRCA1 focus formation. At least 100 cells were counted at each time point. Data were collected from four independent experiments. Error bars represent SEM. **$P < 0.01$; ****$P < 0.0001$.

IRIF, and that BRCA1 PARsylation contributes to the proper dynamics of this process (see the model in Fig. 5).

Non-PARsylated BRCA1 Persists Together with CtIP and BACH1 in IRIF when RAP80 Is Depleted.

We have previously shown that the residual BRCA1 in RAP80-free IRIF colocalizes with the now more abundant HRR-promoting BRCA1-binding proteins CtIP and BACH1 in these cells (15). We, therefore, asked whether inhibiting BRCA1 PARsylation also affects the concentration of CtIP or BACH1 in IRIF. In this regard, BRCA1-D5 appears to bind CtIP more strongly compared with BRCA1-WT, especially after IR-induced DNA damage, possibly through its higher binding affinity for chromatin, in keeping with its failed PARsylation (SI Appendix, Fig. S5A). That said, neither exposing cells to olaparib nor expressing non-PARsylated BRCA1-D5 in cells depleted of endogenous BRCA1 altered the pattern of CtIP or BACH1 concentration in IRIF (Fig. 3 A–D and SI Appendix, Fig. S5 B–F) (21). However, when inhibition of BRCA1 PARsylation with olaparib was combined with RAP80 depletion, the majority of the seemingly "restored" or retained BRCA1 foci contained colocalized CtIP or BACH1 (Fig. 3 A and B and SI Appendix, Fig. S5 B and C).

Similarly, compared with controls, there was significant colocalization of CtIP and HA-BRCA1-D5 staining in the IRIF of RAP80-depleted cells that expressed HA-BRCA1-D5 and had been depleted of endogenous BRCA1-WT (Fig. 3 C and D). A

similar phenotype was observed for colocalization of HA-BRCA1-D5 and BACH1 (SI Appendix, Fig. S5 D and E).

IRIF Localization of BRCA1, RAP80, and CtIP in Human Breast Cancer Cell Lines.

We previously reported that most of 13 breast cancer cell lines examined contained robust levels of RAP80 and PARsylated BRCA1, including T47D, MCF7, and SKBR-3 (21). However, some, such as HCC1143 and MDA-MB231, revealed diminished or undetectable PARsylated BRCA1 despite the presence of comparable levels of unmodified BRCA1. Importantly, one cell line, HCC38, which was derived from a triple-negative breast carcinoma, was deficient in both BRCA1 PARsylation and RAP80 expression (21). Consistent with these observations, many BRCA1-positive, RAP80-free IRIF were present in HCC38 cells (Fig. 4 A and B, where T47D cells serve as a RAP80- and BRCA1 PARsylation-positive control). A significant portion of these HCC38 cells also contained colocalized CtIP (Fig. 4 C and D). Interestingly, HCC1143, another triple-negative carcinoma-derived cell line, while exhibiting moderate RAP80 expression (21), revealed relatively few cells with RAP80-positive IRIF (Fig. 4 A and B). However, these cells included fewer BRCA1/CtIP-positive cells than HCC38 (Fig. 4 C and D). This can be explained by the fact that RAP80, while less abundant in HCC1143 than in several other breast cancer lines, may still bind BRCA1 through the ABRA1 present in these cells and remains biochemically active (21). Thus, despite the absence of proper BRCA1 PARsylation,
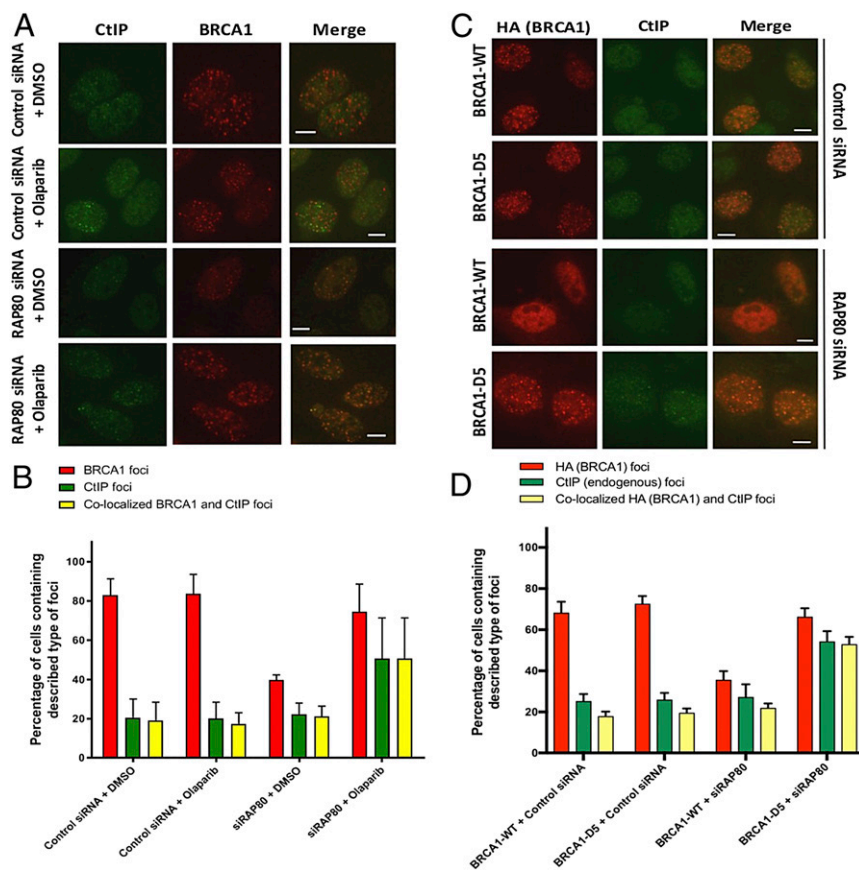
Fig. 3. PARsylation inhibition and RAP80 depletion result in co-concentration of CtIP with BRCA1 in IRIF. (*A*) Representative images showing CtIP and BRCA1 foci formation. Cells were transfected as described in Fig. 2 and then immunostained with antibodies directed against CtIP or BRCA1. (Scale bars, 10 μm.) (*B*) Quantitation of the results in *A*. The graph depicts the percentages of cells containing BRCA1 or CtIP IRIF or those containing foci that contained colocalized BRCA1 and CtIP. (*C*) Representative images showing CtIP and BRCA1 foci formation following ectopic expression of BRCA1-WT/D5 in the presence or absence of RAP80. Cells were immunostained with antibodies directed against CtIP or BRCA1. (Scale bars, 10 μm.) (*D*) Quantitation of results shown in *C*. The figure depicts the percentages of cells containing BRCA1 or CtIP IRIF or those containing foci with colocalized BRCA1 and CtIP. At least 100 cells were counted for each category of foci in each experiment. Data were collected from 3 independent experiments, and error bars indicate SD.
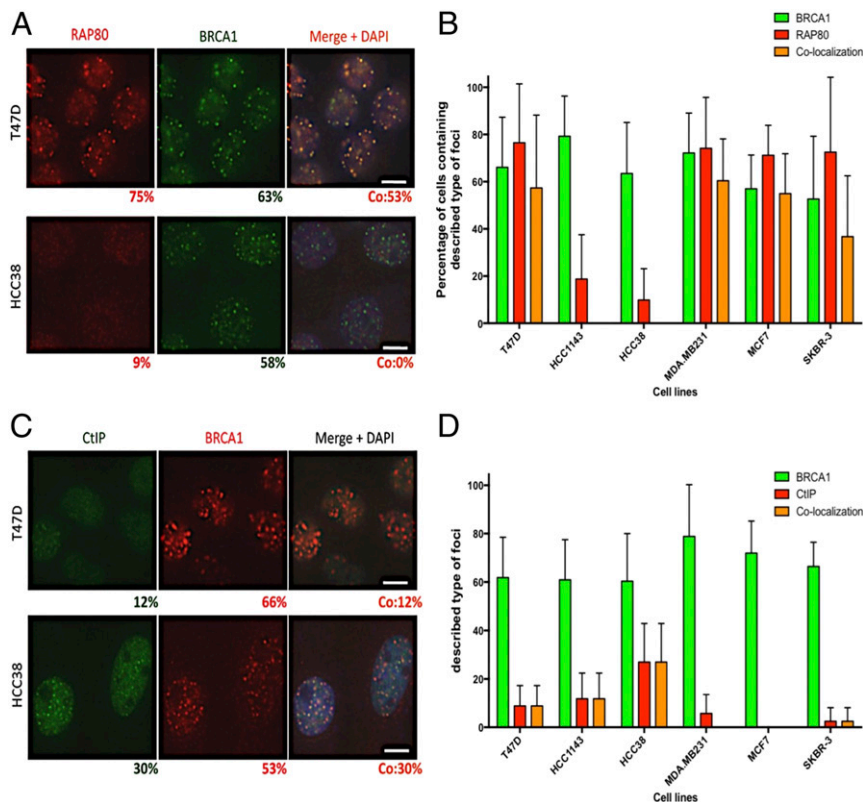
Fig. 4. Formation of BRCA1, RAP80, and CtIP IRIF in T47D and HCC38 cells. (*A*) Representative images showing RAP80 and BRCA1 IRIF formation in T47D or HCC38 cells. The average percentage of cells containing at least 10 RAP80, 10 BRCA1, or colocalized foci is indicated below each respective image. At least 100 cells were counted for each cell line. (Scale bars: 10 μm.) (*B*) Graph showing percentages of cells containing at least 10 RAP80, 10 BRCA1, or RAP80:BRCA1 colocalized foci in 6 breast cancer cell lines. At least 100 cells were counted for each cell line. (*C*) Representative images showing CtIP and BRCA1 IRIF formation in T47D or HCC38 cells. The average percentage of cells containing at least 10 CtIP, 10 BRCA1, or colocalized foci is indicated below each respective image. At least 100 cells were counted for each cell line. (Scale bars: 10 μm.) (*D*) Graph showing the percentages of cells containing at least 10 CtIP, 10 BRCA1, or colocalized foci in 6 human breast cancer cell lines. Data were collected from 2 independent experiments, and error bars indicate SD.

excessive IRIF accumulation of BRCA1-CtIP and BRCA1-BACH1 complexes did not occur, as discussed below.

These results imply that disorderly RAP80- and PARP1-driven BRCA1 HRR regulation can be a clinically relevant phenotype during the development of genomic instability in certain non-familial breast cancers and thus may be an authentic pathophysiological manifestation of breast cancer development.

BRCA1 Overexpression Is Associated with Aneuploidy and Poor Prognosis in Breast Cancers. In a previous paper, we reported that failed BRCA1 PARsylation at a designated residue in its DNA-binding domain led to failed BRCA1 release from chromatin and from IRIF, resulting in the development of high and apparently deregulated HRR activity, which, as we independently found, leads to marked genome instability, multichromosomal structural disorder, and evidence of aneuploidy (21).

In this context, we analyzed the invasive breast cancer cohort in The Cancer Genome Atlas (TCGA) database using a recently developed algorithm for calculating aneuploidy score (35) and found that tumors with higher BRCA1 RNA expression are associated with higher aneuploidy scores (*SI Appendix*, Fig. S6*A*), implying the existence of more prevalent genomic instability in these tumors. Furthermore, in three large analyses of patients with spontaneous, noninherited breast cancer, tumor-based BRCA1 tissue RNA expression was measured and tested for a correlation with relapse-free survival (*SI Appendix*, Fig. S6 *B–D*). In these analyses, it turned out that a higher level of BRCA1 RNA expression, detected in approximately one-half of these patients, was associated with lower relapse-free, overall, and

distant metastasis-free survival than was observed in comparable numbers of patients whose tumors expressed significantly less BRCA1 RNA (*SI Appendix*, Fig. S6 *B–D*). These results imply that abnormally elevated *BRCA1* expression can be associated with a poorer clinical outcome.

In summary, these data reflect correlations between higher-level as opposed to lower-level BRCA1 gene expression and greater tumor-based aneuploidy and a poorer clinical prognosis. One possible explanation for this relationship is that, as suggested in *SI Appendix*, Fig. S6, elevated BRCA1 gene expression, being cell cycle-controlled and normally maximal in S/G2, may well reflect heightened tumor cell proliferation, which is not uncommonly associated with a relatively poor clinical outcome. This notwithstanding, since BRCA1 p220 protein expression and p220 function data were not available in these TCGA datasets, it is difficult to know which, if any, detailed BRCA1 biochemical properties may have contributed to such a negative outcome.

Given that a loss of BRCA1 function is also linked to aberrant biological outcomes, including tumorigenesis, the same amplitude of certain p220 functions may trigger either tumor-suppressing or tumor-promoting outcomes depending on the tissue/organ-based and/or biochemical environment in which it is encountered. Indeed, in this report, we have shown that loss of RAP80 and dysregulation of BRCA1 PARsylation can trigger aneuploidy and genome instability, akin to that associated with tumorigenesis. Thus, these findings represent yet another potential route to tumorigenesis driven, at least in part, by deregulated/hyperactive BRCA1. Interestingly, the results of additional RAP80 analysis,

including a structural study, strongly suggest that it too is a tumor suppressor (36).

Interestingly, recent findings reported by Balmus et al. (37) suggest that excessive HRR activity with end resection, mediated by inactivation of the BRCA1-A complex, is beneficial for ATM-deficient cells, which become resistant to Topoisomerase I and PARP1 inhibitors. These findings, along with the results presented here, provide insight into possible mechanisms by which certain ATM- or BRCA1-mutated cancer cells become resistant to therapeutic agents, the actions of which rely on a normally functioning HRR pathway.

A Model Depicting the Coordinated Functions of the RAP80 Complex and BRCA1 PARsylation in IRIF. PARsylation is a unique post-translational modification induced in response to DNA damage. It is a product of members of a large PARP family, among which PARP1 is the most widely studied. PARP1 is responsible for 90% of DNA damage-induced PARsylation and is first recruited to sites of DNA damage within seconds of damage development, promoting rapid and extensive recruitment of DNA damage response factors to DNA lesions (38).

Among the three best-characterized BRCA1-containing complexes, BRCA1-B (TopBP1/BACH1) and -C (MRN/CtIP) complexes localize to sites of DNA damage mainly through pathways involving PARP1-mediated PARsylation (28) to promote end resection, which can activate HRR (15, 16, 20, 39). On the other hand, the BRCA1-A complex (Abraxas/RAP80), which is phospho-H2AX–dependent, likely accumulates at these DNA damage sites, where it can inhibit end resection (29–31, 40), conceivably via a process mediated by precise protein ubiquitination and deubiquitination (23, 41, 42). Interestingly, we previously showed that BRCA1 is also modified by PARP1, which is required for the stable formation of BRCA1-A (Abraxas/RAP80) complex (21). Nonetheless, how PARP1 and BRCA1 PARsylation operate in balancing these two seemingly counteracting processes remains unclear.

Interestingly, the PARsylated region of BRCA1 does not resemble any of the known PAR-containing modules, such as the PBZ, WWE, FHA, OB-fold, RRM, and PIN domains (43), suggesting that it might operate differently, at least in part. In this regard, others have reported that the BRCT domains of the major BRCA1 partner, BARD1, can bind poly-ADP-ribose, which facilitates the early recruitment of BRCA1/BARD1 heterodimers to DSBs (10, 40).

This process might correspond to the earlier (as opposed to the later) period of BRCA1 PARSylation described in *SI Appendix*, Fig. S3. Conceivably, with its distinctive kinetics, it operates differently from BRCA1 that is parsylated later on. Indeed, despite the fact that BRCA1 is parsylated and there is a possible contribution of these modifications to the integrity of BRCA1/BARD1 heterodimers, non-PARsylated BRCA1-D5 appeared to interact normally with BARD1 (*SI Appendix*, Fig. S5*A*). Thus, it is possible that multiple, temporally nonoverlapping PARsylation events that target BARD1/BRCA1-containing complexes affect their efficient recruitment to sites of DNA damage and the quantity and/or quality of BRCA1 function once bound at these sites.

Based on these considerations, we propose a model centered around the coordinated regulation of BRCA1 PARsylation and the localization of BRCA1 complexes in IRIF. The model is depicted and annotated in Fig. 5. In response to DNA damage, BRCA1 and its pro-HRR partners (i.e., CtIP and BACH1) are recruited to DSB through an RAP80-independent process, as described previously (20, 40). As homologous recombination-mediated DSB repair, supported by pro-HRR BRCA1 complexes (i.e., complexes B and C), is initiated, RAP80 also concentrates in IRIF, where it binds to specific K6- and/or K63-linked polyubiquitin structures located near DSBs (11, 29–31). Conceivably, it exerts its HRR modulation function in this setting.

When present in these multicomponent structures, BRCA1 becomes PARsylated by PARP1 in a process that is likely dynamic. In such a context, PARsylation results in timely BRCA1 release from DNA, at least in part by modifying the BRCA1 DNA-binding domain (21). Moreover, PARsylated BRCA1 is recognized by the RAP80 PAR-interacting domain (PID), which, along with ABRA1, supports the formation of stable BRCA1-A complexes (21). When localized in IRIF, these elements might be viewed, at least in part, as HRR- modulating or anti-HRR structures (15, 19, 20, 23, 44). Therefore, when BRCA1 complex binding to and release from chromatin is accomplished in proper order, physiological loading and unloading of pro- and anti-HRR complexes likely occurs in IRIF to insure HRR regulation without a breakdown in chromosomal integrity. In this model, BRCA1 would remain in IRIF, despite a change in its major partner protein repertoire (from CtIP/BACH1 to RAP80/ABRA1) (Fig. 5, first box).

In RAP80-depleted cells, BRCA1 can still be PARsylated by PARP1. However, PARsylated BRCA1 cannot interact with the
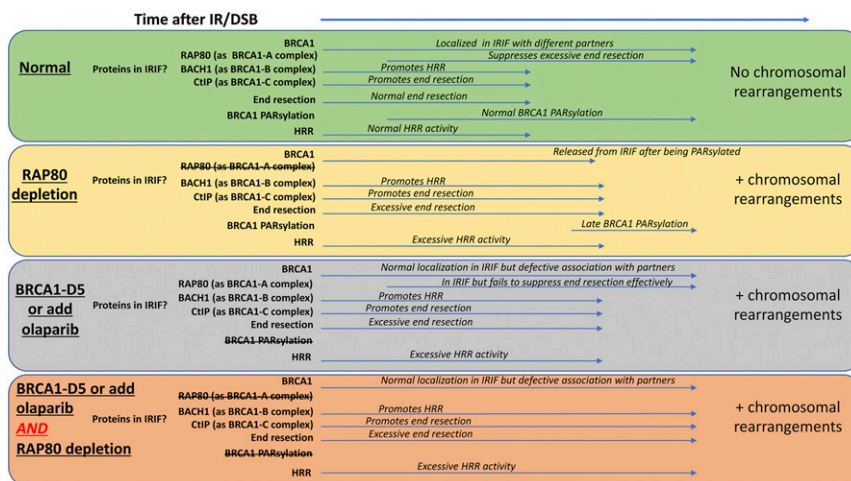
Fig. 5. Model depicting the HRR tuning process in which BRCA1 PARsylation and RAP80 function together to regulate the normal presence of BRCA1 and its partner proteins in IRIF and to suppress chromosome instability. The substance of this figure is described and analyzed in the text.

now-absent RAP80, allowing a gradual loss of BRCA1 from chromatin (see below). In addition, it is likely that after forced depletion, RAP80 is lost from core IRIF segments, thereby allowing DNA end resection to occur at DSBs concentrated therein beyond the normal boundary (19, 20, 23). This likely results in excessive HRR.

Thus, the gradual loss of BRCA1 after IR from most foci in the absence of RAP80 is not a result of BRCA1 recruitment failure, but rather is a manifestation of a defective HRR tuning process that occurs when RAP80 is absent but the later component of BRCA1 PARsylation remains intact (Fig. 5, second box). Similarly, in cells treated with olaparib or expressing the non-PARsylatable BRCA1-D5 mutant despite the normal localization of BRCA1 and RAP80 in IRIF, without proper BRCA1 PARsylation, stable BRCA1-A complex fails to form, as we reported previously (21). As a result, excessive end resection and HRR also occur (Fig. 5, third box).

Indeed, when cells are both deprived of RAP80 and cannot PARsylate BRCA1, un-PARsylated BRCA1 cannot depart the DNA with the same kinetics as when it is properly PARsylated. In the absence of RAP80, pro-HRR BRCA1 complexes are much more visually prominent in IRIF where they can be retained for longer than normal periods. These effects and the absence of a RAP80-driven limitation of DSB end resection are associated with a marked hyper-HRR phenotype, which we propose to be a result of a major failure of the HRR tuning mechanism (Fig. 5, fourth box).

Conceivably, excessive accumulation of active BRCA1-B and -C complexes in IRIF trigger excessive DNA end resection, a CtIP-dependent process (45), along with nonallelic recombination and/or the formation of irresolvable recombination intermediates (44, 46, 47). It might also interfere with the activation of BRCA1- mediated S/G2 checkpoints (20). These developments could lead to additional DNA breakage, chromosomal rearrangements, and overt genomic instability reminiscent of alterations that contribute to carcinogenesis.

Methods

Plasmids, DNA Constructs and Antibodies. All plasmids and recombinant plasmids used in this study have been described previously (15, 21). The following antibodies were used in immunoprecipitation, Western blot (WB), and immunofluorescence (IF) experiments: rabbit polyclonal anti-RAP80 (Bethyl Laboratories; 1:1,000 for WB and IF), rabbit polyclonal anti-RAP80 (H-260; Santa Cruz Biotechnology), mouse monoclonal anti-PARP1 (clone C2-10; Trevigen and BD Pharmingen; 1:1,000 for WB), mouse monoclonal anti-PARP1 (clone 4C10-5; BD Pharmingen; 1:500 for WB), rabbit polyclonal anti-BRCA1 (EMD Millipore; 1:2,500 for WB and IF), mouse monoclonal anti-BRCA1 (MS110, Millipore OP92, 1:50 for WB), mouse monoclonal anti-BRCA1 (D9; Santa Cruz Biotechnology; 1:50 for IF), rabbit polyclonal anti-BRCA1 (A300-000; Bethyl Laboratories), mouse monoclonal anti-mouse BRCA1 (GH118, made in house, 1:50 for WB) (48), rabbit polyclonal anti-BACH1 (Sigma-Aldrich; 1:1,000 for WB), mouse monoclonal anti-BACH1 (1:10 for IF, kind gift from Sharon Cantor, University of Massachusetts Medical School, Worcester, MA) (49), rabbit polyclonal anti-CtIP (Bethyl Laboratories; 1:1,000 for WB), mouse monoclonal anti-CtIP (1:40 for IF, kind gift from Richard Baer, Columbia University, New York, NY) (50), mouse monoclonal anti-HA (HA.11; Covance; 1:1,000 for WB), and rabbit polyclonal anti-Abraxas (N2; made in house, 1:2,000 for WB) (15).

I-SceI Recombination Assay. U2OS cells containing a single copy of the *DR-GFP* reporter (U2OS-DR) were used following a previously described methodology (51).

Cell Culture. All cells were cultivated at 37 °C in a humidified incubator in an atmosphere containing 10% CO_2. U2OS cells were grown in DMEM supplemented with 10% FBS. Breast cancer cell lines were cultured according to the guidelines provided by American Type Culture Collection or the suppliers.

RNA Interference. The following siRNA or shRNA sequences were used in this study:

siBRCA1-1: AGAUAGUUCUACCAGUAAA

siBRCA1-2: GAAUCCUAGAGAUACUGAA

siPARP1-1: CCAAAGGAAUUCCGAGAAA

siPARP1-2: CCGAGAAAUCUCUUACCUCAA

siPARP1-3: ACGGUGAUCGGUAGCAACAAA

siTP53BP1: GGACUCCAGUGUUGUCAUU

shLuciferase: GTGCGCTGCTGGTGCCAAC

shBRCA1-1: AGAATCCTAGAGATACTGAA

shBRCA1-2: TATAAGACCTCTGGCATGAAT

shPARP1: AAGGTGGTTGACAGAGATTCT

Nontargeting siRNA pools from Dharmacon were used as siRNA controls, and shRNA targeting luciferase was used as an shRNA control in all experiments. siRNA transfections were performed using HiPerFect (Qiagen) or Lipofectamine RNAiMax (Invitrogen) according to the manufacturer's instructions.

Chromosome Analysis. U2OS cells were exposed to the indicated siRNA or drugs or were transfected with an indicated cDNA for 48 h and then exposed to 150 rads of IR. At 5 h after IR, 30 ng/mL colcemid was added to each culture, and cells were incubated for an additional 3 h, collected, and then prepared for an analysis of metaphase spreads. Spreads were stained with DAPI.

Immunofluorescence. Immunofluorescence following irradiation was performed as described previously (31, 52).

Data Availability. All of the data supporting the findings of this study are available within the paper and *SI Appendix*.

1. R. D. Johnson, M. Jasin, Sister chromatid gene conversion is a prominent double-strand break repair pathway in mammalian cells. *EMBO J.* **19**, 3398–3407 (2000).
2. R. D. Johnson, M. Jasin, Double-strand break-induced homologous recombination in mammalian cells. *Biochem. Soc. Trans.* **29**, 196–201 (2001).
3. C. J. Shaw, J. R. Lupski, Implications of human genome architecture for rearrangement-based disorders: The genomic basis of disease. *Hum. Mol. Genet.* **13**, R57–R64 (2004).
4. L. Wu, I. D. Hickson, The Bloom's syndrome helicase suppresses crossing over during homologous recombination. *Nature* **426**, 870–874 (2003).
5. K. Gari, C. Décaillet, A. Z. Stasiak, A. Stasiak, A. Constantinou, The Fanconi anemia protein FANCM can promote branch migration of Holliday junctions and replication forks. *Mol. Cell* **29**, 141–148 (2008).
6. K. Fugger et al., Human Fbh1 helicase contributes to genome maintenance via pro- and anti-recombinase activities. *J. Cell Biol.* **186**, 655–663 (2009).
7. G. L. Moldovan et al., Inhibition of homologous recombination by the PCNA-interacting protein PARI. *Mol. Cell* **45**, 75–86 (2012).
8. Y. Hu et al., RECQL5/Recql5 helicase regulates homologous recombination and suppresses tumor formation via disruption of Rad51 presynaptic filaments. *Genes Dev.* **21**, 3073–3084 (2007).
9. L. J. Barber et al., RTEL1 maintains genomic stability by suppressing homologous recombination. *Cell* **135**, 261–271 (2008).
10. J. Her, N. Soo Lee, Y. Kim, H. Kim, Factors forming the BRCA1-A complex orchestrate BRCA1 recruitment to the sites of DNA damage. *Acta Biochim. Biophys. Sin. (Shanghai)* **48**, 658–664 (2016).
11. B. Wang et al., Abraxas and RAP80 form a BRCA1 protein complex required for the DNA damage response. *Science* **316**, 1194–1198 (2007).
12. M. H. Yun, K. Hiom, CtIP-BRCA1 modulates the choice of DNA double-strand break repair pathway throughout the cell cycle. *Nature* **459**, 460–463 (2009).
13. R. Litman et al., BACH1 is critical for homologous recombination and appears to be the Fanconi anemia gene product FANCJ. *Cancer Cell* **8**, 255–265 (2005).
14. W. Zhao et al., BRCA1-BARD1 promotes RAD51-mediated homologous DNA pairing. *Nature* **550**, 360–365 (2017).
15. Y. Hu et al., RAP80-directed tuning of BRCA1 homologous recombination function at ionizing radiation-induced nuclear foci. *Genes Dev.* **25**, 685–700 (2011).
16. K. A. Coleman, R. A. Greenberg, The BRCA1-RAP80 complex regulates DNA repair mechanism utilization by restricting end resection. *J. Biol. Chem.* **286**, 13669–13680 (2011).

17. S. M. Dever *et al.*, Mutations in the BRCT-binding site of BRCA1 result in hyper-recombination. *Aging (Albany N.Y.)* **3**, 515–532 (2011).
18. S. D. Dimitrov *et al.*, Physiological modulation of endogenous BRCA1 p220 abundance suppresses DNA damage during the cell cycle. *Genes Dev.* **27**, 2274–2291 (2013).
19. A. Kakarougkas *et al.*, Co-operation of BRCA1 and POH1 relieves the barriers posed by 53BP1 and RAP80 to resection. *Nucleic Acids Res.* **41**, 10298–10311 (2013).
20. M. Goldstein, M. B. Kastan, Repair versus checkpoint functions of BRCA1 are differentially regulated by site of chromatin binding. *Cancer Res.* **75**, 2699–2707 (2015).
21. Y. Hu *et al.*, PARP1-driven poly-ADP-ribosylation regulates BRCA1 function in homologous recombination-mediated DNA repair. *Cancer Discov.* **4**, 1430–1447 (2014).
22. P. Rouet, F. Smih, M. Jasin, Introduction of double-strand breaks into the genome of mouse cells by expression of a rare-cutting endonuclease. *Mol. Cell. Biol.* **14**, 8096–8106 (1994).
23. D. Typas *et al.*, The de-ubiquitylating enzymes USP26 and USP37 regulate homologous recombination by counteracting RAP80. *Nucleic Acids Res.* **43**, 6919–6933 (2015). Correction in: *Nucleic Acids Res.* **44** 2976 (2016).
24. B. Adamson, A. Smogorzewska, F. D. Sigoillot, R. W. King, S. J. Elledge, A genome-wide homologous recombination screen identifies the RNA-binding protein RBMX as a component of the DNA-damage response. *Nat. Cell Biol.* **14**, 318–328 (2012).
25. K. A. Menear *et al.*, 4-[3-(4-cyclopropanecarbonylpiperazine-1-carbonyl)-4-fluorobenzyl]-2H-phthalazin-1-one: A novel bioavailable inhibitor of poly(ADP-ribose) polymerase-1. *J. Med. Chem.* **51**, 6581–6591 (2008).
26. P. Bouwman *et al.*, 53BP1 loss rescues BRCA1 deficiency and is associated with triple-negative and BRCA-mutated breast cancers. *Nat. Struct. Mol. Biol.* **17**, 688–695 (2010).
27. S. F. Bunting *et al.*, 53BP1 inhibits homologous recombination in Brca1-deficient cells by blocking resection of DNA breaks. *Cell* **141**, 243–254 (2010).
28. C. Liu, A. Vyas, M. A. Kassab, A. K. Singh, X. Yu, The role of poly ADP-ribosylation in the first wave of DNA damage response. *Nucleic Acids Res.* **45**, 8129–8141 (2017).
29. H. Kim, J. Chen, X. Yu, Ubiquitin-binding protein RAP80 mediates BRCA1-dependent DNA damage response. *Science* **316**, 1202–1205 (2007).
30. J. Yan *et al.*, The ubiquitin-interacting motif containing protein RAP80 interacts with BRCA1 and functions in DNA damage repair response. *Cancer Res.* **67**, 6647–6656 (2007).
31. B. Sobhian *et al.*, RAP80 targets BRCA1 to specific ubiquitin structures at DNA damage sites. *Science* **316**, 1198–1202 (2007).
32. Z. Yin *et al.*, RAP80 is critical in maintaining genomic stability and suppressing tumor development. *Cancer Res.* **72**, 5080–5090 (2012).
33. J. Murai *et al.*, Trapping of PARP1 and PARP2 by clinical PARP inhibitors. *Cancer Res.* **72**, 5588–5599 (2012).
34. M. Zimmermann *et al.*, CRISPR screens identify genomic ribonucleotides as a source of PARP-trapping lesions. *Nature* **559**, 285–289 (2018).
35. A. M. Taylor *et al.*, Genomic and functional approaches to understanding cancer aneuploidy. *Cancer Cell* **33**, 676–689.e3 (2018).
36. J. Nikkilä *et al.*, Familial breast cancer screening reveals an alteration in the RAP80 UIM domain that impairs DNA damage response function. *Oncogene* **28**, 1843–1852 (2009).
37. G. Balmus *et al.*, ATM orchestrates the DNA-damage response to counter toxic non-homologous end-joining at broken replication forks. *Nat. Commun.* **10**, 87 (2019).
38. J. F. Haince *et al.*, PARP1-dependent kinetics of recruitment of MRE11 and NBS1 proteins to multiple DNA damage sites. *J. Biol. Chem.* **283**, 1197–1208 (2008).
39. A. Cruz-García, A. López-Saavedra, P. Huertas, BRCA1 accelerates CtIP-mediated DNA-end resection. *Cell Rep.* **9**, 451–459 (2014).
40. M. Li, X. Yu, Function of BRCA1 in the DNA damage response is mediated by ADP-ribosylation. *Cancer Cell* **23**, 693–704 (2013).
41. Y. Li *et al.*, USP13 regulates the RAP80-BRCA1 complex-dependent DNA damage response. *Nat. Commun.* **8**, 15752 (2017).
42. K. Baranes-Bachar *et al.*, The ubiquitin E3/E4 ligase UBE4A adjusts protein ubiquitylation and accumulation at sites of DNA damage, facilitating double-strand break repair. *Mol. Cell* **69**, 866–878.e7 (2018).
43. H. Wei, X. Yu, Functions of PARylation in DNA damage repair pathways. *Genomics Proteomics Bioinformatics* **14**, 131–139 (2016).
44. J. Lukas, C. Lukas, J. Bartek, More than just a focus: The chromatin response to DNA damage and its role in genome integrity maintenance. *Nat. Cell Biol.* **13**, 1161–1169 (2011).
45. A. A. Sartori *et al.*, Human CtIP promotes DNA end resection. *Nature* **450**, 509–514 (2007).
46. R. Colnaghi, G. Carpenter, M. Volker, M. O'Driscoll, The consequences of structural genomic alterations in humans: Genomic disorders, genomic instability and cancer. *Semin. Cell Dev. Biol.* **22**, 875–885 (2011).
47. C. A. Adelman, S. J. Boulton, Metabolism of postsynaptic recombination intermediates. *FEBS Lett.* **584**, 3709–3716 (2010).
48. S. Ganesan *et al.*, BRCA1 supports XIST RNA concentration on the inactive X chromosome. *Cell* **111**, 393–405 (2002).
49. S. B. Cantor *et al.*, BACH1, a novel helicase-like protein, interacts directly with BRCA1 and contributes to its DNA repair function. *Cell* **105**, 149–160 (2001).
50. X. Yu, R. Baer, Nuclear localization and cell cycle-specific expression of CtIP, a protein that associates with the BRCA1 tumor suppressor. *J. Biol. Chem.* **275**, 18541–18549 (2000).
51. B. Xia *et al.*, Control of BRCA2 cellular and clinical functions by a nuclear partner, PALB2. *Mol. Cell* **22**, 719–729 (2006).
52. R. A. Greenberg *et al.*, Multifactorial contributions to an acute DNA damage response by BRCA1/BARD1-containing complexes. *Genes Dev.* **20**, 34–46 (2006).

MEDICAL SCIENCES